Hierarchical Patterning of Multifunctional Conducting Polymer Nanoparticles as a Bionic Platform for Topographic Contact Guidance

Dominic Ho,[†,‡] Jianli Zou,[§] Xianjue Chen,[†,□] Alaa Munshi,[†] Nicole M. Smith,[†,∥] Vipul Agarwal,[†] Stuart I. Hodgetts,[‡] Giles W. Plant,[⊥] Anthony J. Bakker,[‡] Alan R. Harvey,[‡] Igor Luzinov,[#] and K. Swaminathan Iyer*[,†]

[†]School of Chemistry and Biochemistry, The University of Western Australia, Crawley, Western Australia 6009, Australia, [‡]School of Anatomy, Physiology and Human Biology, The University of Western Australia, Crawley, Western Australia 6009, Australia, [§]Institute for Integrated Cell-Material Sciences (iCeMS), iCeMS Complex 2, Kyoto University, Yoshida-Honmachi, Sakyo-ku, Kyoto, 606-8501, Japan, [∥]Experimental and Regenerative Neurosciences, School of Animal Biology, The University of Western Australia, Crawley, Western Australia 6009, Australia, [⊥]Stanford Partnership for Spinal Cord Injury and Repair, Department of Neurosurgery, Stanford University School of Medicine, Stanford, California 94305, United States, and [#]School of Materials Science and Engineering, Clemson University, Clemson, South Carolina 29634, United States. [□]Present address: Centre for NanoScale Science and Technology, School of Chemical and Physical Sciences, Flinders University, Bedford Park, Adelaide, SA 5042, Australia.

ABSTRACT The use of programmed electrical signals to influence biological events has been a widely accepted clinical methodology for neurostimulation. An optimal biocompatible platform for neural activation efficiently transfers electrical signals across the electrode–cell interface and also incorporates large-area neural guidance conduits. Inherently conducting polymers (ICPs) have emerged as frontrunners as soft biocompatible alternatives to traditionally used metal electrodes, which are highly invasive and elicit tissue damage over long-term implantation. However, fabrication techniques for the ICPs suffer a major bottleneck, which limits their usability and medical translation. Herein, we report that these limitations can be overcome using colloidal chemistry to fabricate multimodal conducting polymer nanoparticles. Furthermore, we demonstrate that these polymer nanoparticles can be precisely assembled into large-area linear conduits using surface chemistry. Finally, we validate that this platform can act as guidance conduits for neurostimulation, whereby the presence of electrical current induces remarkable dendritic axonal sprouting of cells.

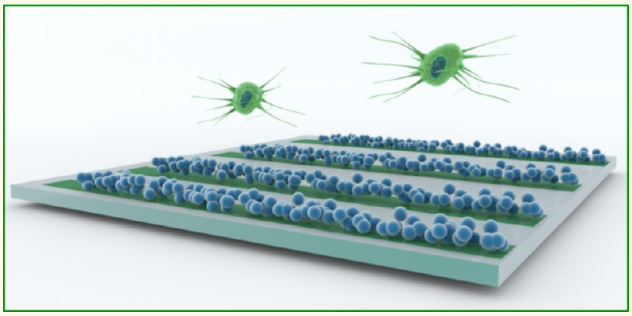

KEYWORDS: multimodal nanoparticles · conducting polymers · capillary force lithography · neurostimulation

Exogenous electrical stimulation has been effectively used both in clinical practice and in laboratory research to regulate cell-type-dependent adhesion, differentiation, and growth.[1] This phenomenon of introducing programmed electrical signals locally to influence biological events has resulted in the pursuit of sophisticated medical bionic devices.[2] An important property that dictates the performance of most bionic electrodes is the electrode/cellular interface and its ability to transmit charge across the biointerface.[3] Traditionally metallic electrodes made of platinum, gold, iridium oxide, tungsten, their alloys, and more recently carbon fibers have been effectively employed in bionic devices.[4] They have been employed for deep brain stimulation, as cochlear implants, for vagus nerve stimulation to treat epilepsy, and for stimulating regeneration in the central nervous system.[2] However, stiff metal electrodes suffer a major drawback of eliciting tissue damage over long-term implantation.[2] Importantly, it is now recognized that nanoscale patterns provide topographic guidance cues for cells. This has been widely exploited to engineer sophisticated regenerative platforms for nerves, muscles, skin, and bones.[5] The need to incorporate large-area nanoscale patterns for bionic applications coupled with the demand toward miniaturization of

* Address correspondence to swaminatha.iyer@uwa.edu.au.

Received for review November 20, 2014 and accepted January 26, 2015.

Published online January 26, 2015
10.1021/nn506607x

biocompatible implantable devices has resulted in the emergence of inherently conducting polymers as frontrunners for fabricating flexible organic electrode materials. However, advances in the applicability of patterned surfaces of inherently conducting polymers in bionic devices have been limited due to the difficulties of transferring printing techniques and their integration under physiological conditions. In this article, we report a transferable method to fabricate multifunctional poly(3,4-ethylenedioxythiophene)-poly(styrenesulfonate) (PEDOT:PSS) nanoparticles and direct their self-assembly by electrostatic interactions into large-area patterns. Using the rat pheochromocytoma cell line (PC12), we demonstrate the suitability of the assembly as a bionic platform for exogenous electrical stimulation.

The three primary classes of conducting polymers that have been studied are polyanilines, polypyrroles, and polythiophenes.[6] The ease of functionalization of polythiophenes and maintenance of conductivity under physiological conditions has made them primary candidates for multifunctional organic bionic devices.[7] The most widely explored processes for the fabrication of organic conducting polymer patterns are electropolymerization, extrusion printing, inkjet printing, microcontact printing, electrospinning, and more recently high-precision Dip Pen Nanolithography (DPN).[4,6] Electropolymerization has been widely used for coating metal/carbon substrates, following which patterning is achieved by top-down lithography on polymer thin films covering larger area electrodes. This technique results in controlled, high-resolution nanoscale patterns but is limited by the ability to regulate polymerization of monomers on nanoscale implantable electrodes.[8] Similarly, printing techniques have achieved significant advances in recent years, reaching high-throughput patterns, but are limited in resolution by the liquid dispensing techniques, which operate within the limit of tens of micrometers.[9] Electrospinning techniques have offered simple processable solutions to generate 3D scaffolds at resolutions mimicking the extracellular matrix architecture but are limited by the inability to generate patterned conducting conduits for the development of bionic guidance channels.[4] The aforementioned shortfalls have been recently overcome by the advances of DPN, which enables precise deposition, patterning down to nanoscale resolution, and most importantly applicability over a wide range of substrates.[10] However, advances are limited by their cost, need for specialized equipment, and low throughput. In the present paper we adopt a bottom-up self-assembly process to precisely pattern conducting polymer nanoparticles into patterns as conduits for guidance. The approach is easily adoptable over multiple substrates, needs no specialized equipment, and affords large-area patterns. Importantly, this approach enables drug encapsulation and sustained release from the nanoparticles once patterned and multimodal imaging of the nanoparticle constructs once implanted.

RESULTS AND DISCUSSION

Patterned Multifunctional PEDOT:PSS Nanoparticle Arrays. In this study poly(glycidal methacrylate) (PGMA) is used as a reactive macromolecular anchoring platform both on the substrate as a nanoscale layer and as a colloidal nanoparticle to enable multilayer assembly (Figure 1). A polymer with epoxy functionality was chosen, since the reactions of epoxy groups are universal and easily transferable to various substrates, affording ease of attachment of functional molecules. Furthermore, the epoxy groups of the polymer can cross-link to provide structural integrity to the pattern and nanoparticle constructs.[11] The mobility of the reactive loops of PGMA ensures greater access to anchoring, resulting in a 2−3-fold greater grafting density when compared to a monolayer of epoxy groups on a nanoparticle surface of similar dimension, enabling high loading using a layer by layer approach that is adopted in the current study.[11] Polymer nanospheres were initially prepared using an oil in water emulsion methodology from PGMA modified with a rhodamine-B (RhB) dye, encapsulated with magnetite (Fe_3O_4) nanoparticles to form the core platform (Figure 1a,b). Not only does the incorporation of magnetite and RhB render these constructs multimodal for both MRI and fluorescence imaging, but importantly in the present case magnetite provides a means to separate, wash, and purify the nanoparticles using a magnetic fractionation column during each step of layered assembly. Polyethylenimine (PEI) was then covalently bound to the RhB-PGMA core to facilitate a cationic layer for electrostatic conjugation of an anionic conducting polymer, PEDOT:PSS (Figure 1c,d). Capillary force lithography (CFL) was then used to generate large-area nanoscale conduits in which PEDOT:PSS nanoparticles are electrostatically directed to self-assemble as linear channels from solution (Figure e,f). Capillarity allows the polymer melt to fill up the void space between the polymer and the applied mold when the temperature is above the glass-transition temperature (T_g), thereby generating a large-area pattern that depends on the size of stamp. Importantly, the technique needs no specialized instrumentation for generation of large-area patterns. Patterns can easily be generated using polydimethylsiloxane (PDMS) stamps, which in turn can be fabricated using the ubiquitous optical storage discs as a master. An optical data storage disc is typically made of a polymer (polycarbonate) disc, on which a single spiral track is drilled. The typical width and depth of each line in the spiral track are 800 and 130 nm, respectively, and the periodicity of the track is ~1.5 μm (Figure S1). In the present study, an indium tin oxide (ITO) substrate was

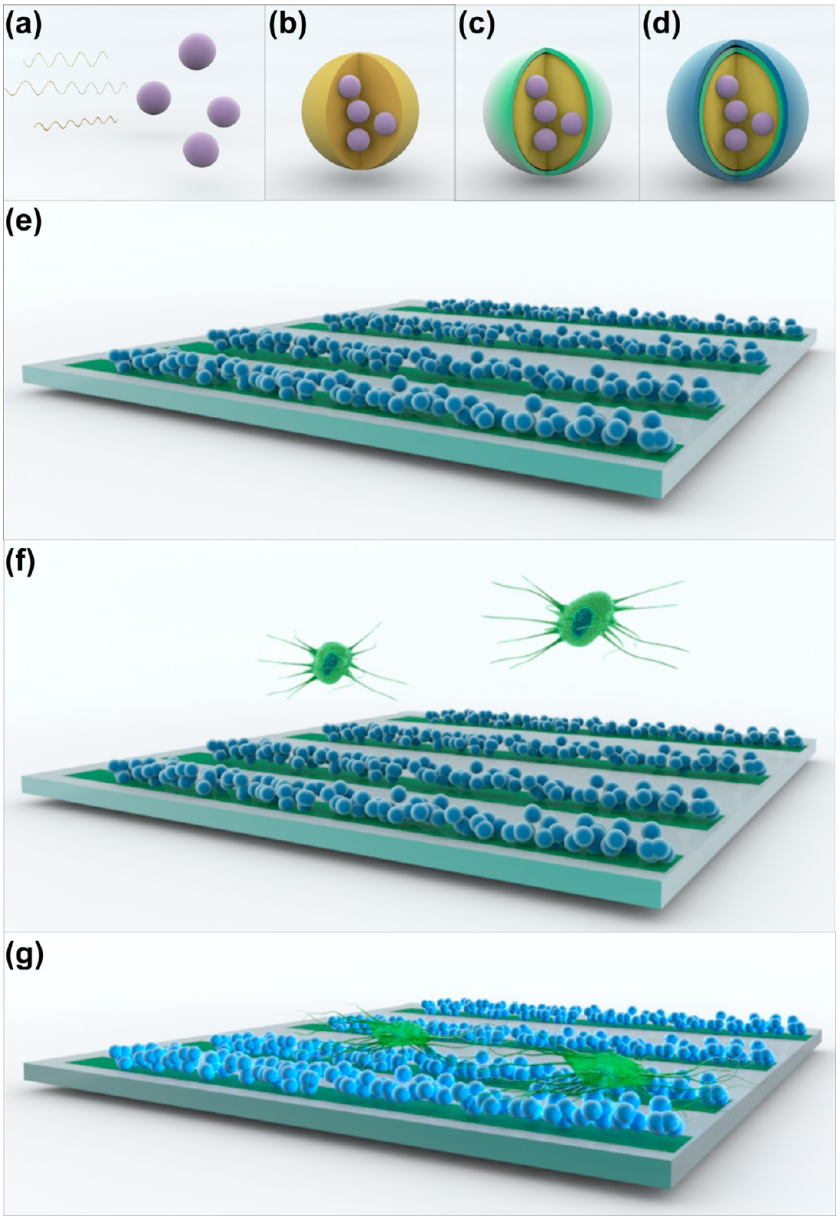

Figure 1. Schematic illustration of the fabrication protocol to pattern multifunctional PEDOT:PSS nanoparticle arrays for exogenous electrical stimulation. (a−d) Multilayer assembly of conducting PEDOT:PSS nanoparticle fabrication *via* non-spontaneous emulsification. (a) An organic phase is initially formed by dissolving RhB-modified PGMA (yellow) and Fe_3O_4 (purple) in a 1:3 mixture of $CHCl_3$ and MEK. (b) Colloidal fluorescent PGMA-Fe_3O_4 nanoparticles are fabricated upon dropwise addition of the organic phase to an aqueous solution of Pluronic F-108. (c) Cationic second layer *via* covalent attachment of PEI (green) to the PGMA-Fe_3O_4 core. (d) Anionic conducting polymer layer *via* electrostatic attachment of PEDOT:PSS (blue). (e−g) Patterning of the multilayered PEDOT:PSS nanoparticles for exogenous electrical stimulation of PC12 cells. (e) Linear nanoparticle conduits patterned on a substrate *via* capillary force lithography (CFL) using charge complementarity. A detailed schematic of the CFL procedure can be found in Figure S2. (f) PC12 cells (green) were cultured onto the biocompatible platform, followed by (g) exogenous electrical modulation.

modified first by spin coating a thin film of PGMA followed by a second spin-coated layer of polystyrene (PS) using previously reported conditions.[12] The PS layer acts as a chemical resist to selectively react the epoxy groups of PGMA following patterning. The PS/PGMA bilayer was annealed with the PDMS mask at 130 °C ($T > T_g$ of PS) to induce patterning *via* capillary flow. The reusable PDMS stamp was peeled off following heat treatment to obtain a patterned surface resulting in alternating PGMA and PS stripes. Ethylenediamine (EA) was then grafted to PGMA to result in cationic linear patterns. PEDOT:PSS nanoparticles were then electrostatically assembled onto the patterned surface, followed by washing steps to remove PS to obtain linear arrays of assembled PEDOT:PSS nanoparticles. A detailed schematic of the fabrication process is shown in Figure S2. The nanoparticle and the patterns were characterized at each step of the assembly (Figure 2). The PEDOT:PSS nanoparticles were an average size of 200 nm (Z-average) with a

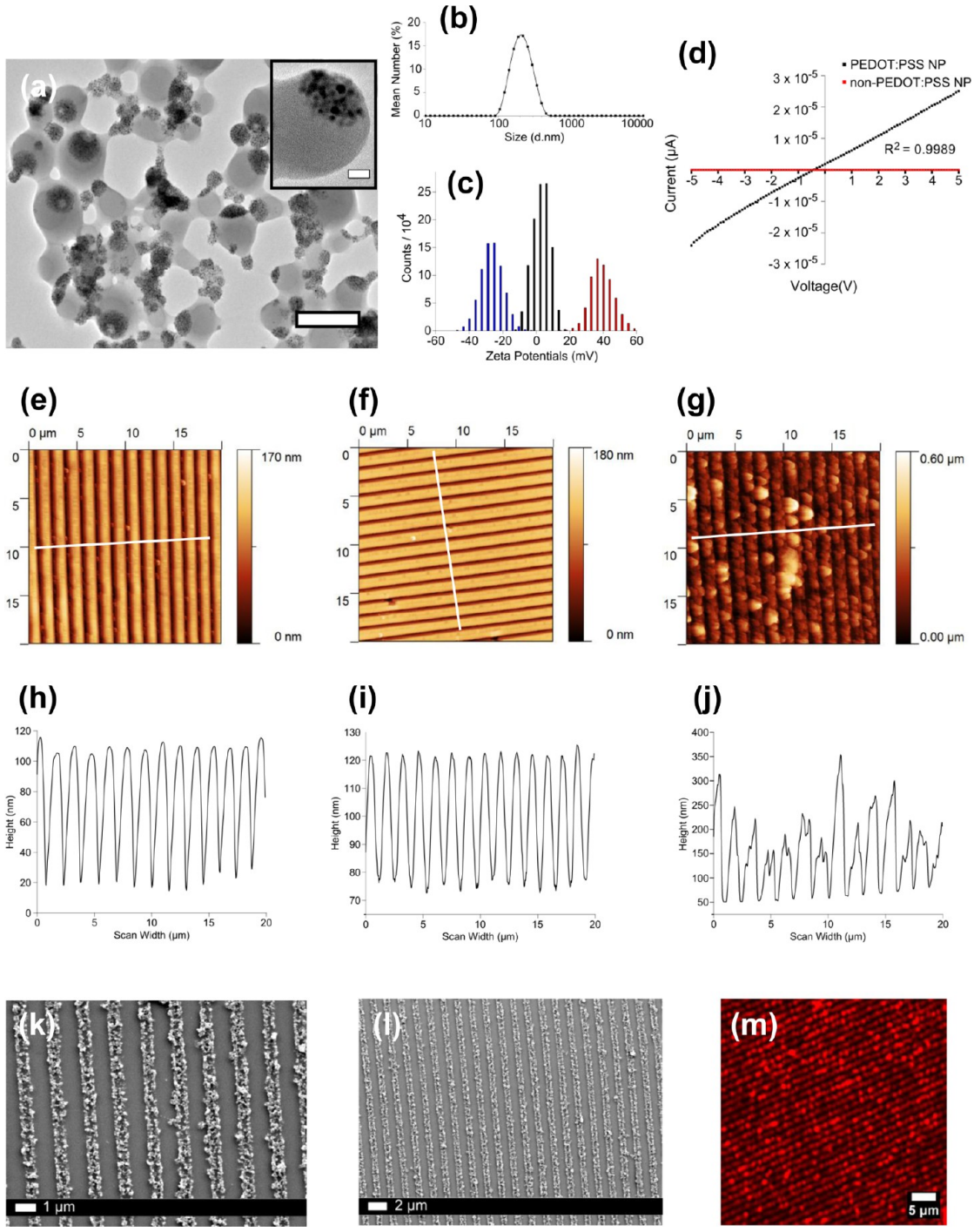

Figure 2. Characterization of the multilayered PEDOT:PSS conducting nanoparticles and their assembly as linear conduits. (a) TEM micrograph of the multilayered PEDOT:PSS nanoparticles. Scale bar = 200 nm. (Inset: high-magnification TEM image of PEDOT:PSS-coated nanoparticles showing encapsulated Fe_3O_4 nanoparticles. Scale bar = 10 nm.) (b) DLS particle size distributions of the PEDOT:PSS nanoparticles in solution. (c) Zeta potential distributions of the nanoparticles: PGMA-Fe_3O_4 core (black) with an average zeta potential of 3.9 $\pm$ 1.3 mV, cationic PEI-coated (red) with an average zeta potential of 37 $\pm$ 1.2 mV, and anionic PEDOT:PSS-coated (blue) with an average zeta potential of -29 ± 6.15 mV. (d) Current *vs* voltage response for the nonconducting PEI-coated nanoparticles (red) and conducting PEDOT:PSS-coated (black) nanoparticles. (e–g) Tapping mode AFM topography images of the nanoparticle patterns at each stage of fabrication: PGMA and PS stripes (e), EA-modified PGMA and PS stripes (f), PEDOT:PSS nanoparticle patterns (g). (h–j) Corresponding height profiles of the nanoparticle patterns at each stage of fabrication.: PGMA and PS stripes (h), EA-grafted PGMA and PS stripes (i), PEDOT:PSS nanoparticles patterns (j). The AFM line scans corresponding to the height profiles are indicated on the topography images in (e)–(g). (k, l) SEM micrographs of the nanoparticle patterns at a magnification of 25k$\times$ (k) and 11k$\times$ (l) indicating the formation of tightly packed and highly ordered nanoparticle arrays. (m) Confocal fluorescence image of the RhB-functionalized PEDOT:PSS nanoparticle arrays at 20$\times$ magnification.

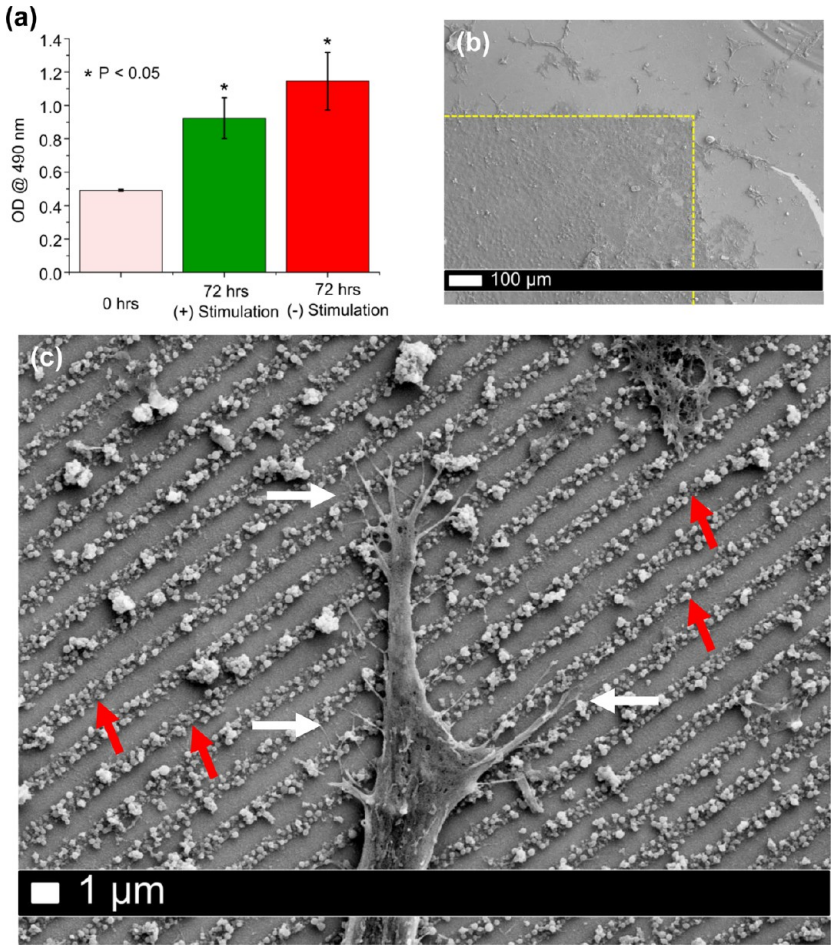

Figure 3. Biocompatibility of the PEDOT:PSS nanoparticle arrays with PC12 cells. (a) Cell viability determined using MTS calorimetric assay obtained at 72 h after an initial exogenous electrical stimulation for 2 h and in the absence of stimulation showing no significant changes. (b) SEM micrograph demonstrating preferential cell adhesion to the pattern area (yellow box). Image acquired at 323× magnification 72 h after the addition of NGF without exogenous electrical stimulation. (c) High-magnification (12k× magnification) SEM images demonstrating specific and preferential interactions of neurites (white arrows) with the PEDOT:PSS linear conduits (red arrows).

polydispersity index (PDI) of 0.07, a zeta potential of -29 ± 6.15 mV, and a conductivity of 2.5×10^{-12} S/cm. The measured conductivity is in accordance with other values reported in the literature for polymer blends.[13] Importantly, this low conductivity is important under physiological conditions to induce local cellular stimulation and avoid tissue damage due to toxic overstimulation.[14] The final self-assembled linear arrays of PEDOT:PSS nanoparticles were of large-area high-density packing, as confirmed at various length scales using AFM, SEM, and fluorescence imaging.

Biocompatibility Assessment of the PEDOT:PSS Nanoparticle Arrays. Topographic modulation of tissue response is one of the most important considerations in developing bionic implants. Topographic contact guidance using micropatterns has been widely exploited to influence cell migration, adhesion, and proliferation.[15,16] One of the pivotal first steps in the present study was to establish biocompatibility of the patterned structures. PC12 cells were chosen in the present case, as they have been demonstrated to show enhanced neurite outgrowth and spreading upon exogenous stimulation on a conducting polymer substrate.[17] MTS (3-(4,5-dimethylthiazol-2-yl)-5-(3-carboxymethoxyphenyl)-2-(4-sulfophenyl)-2*H*-tetrazolium, inner salt) assays, cell viability assays, and SEM imaging were performed after exogenous electrical stimulation and in the absence of electrical stimulation to determine effects on cell viability and cell adhesion (Figure 3a,b and Figure S3). The stimulation conditions used in the present study involved a monophasic pulsed current at a frequency of 250 Hz with a 2 ms pulse width and an amplitude of 1 mA for 2 h, similar to protocols previously reported for similar cell lines.[18,19] Importantly, we observed no changes in cell viability upon exogenous stimulation and observed preferential adhesion of the PC12 cells to the patterned surface over a nonpatterned surface in both cases (± stimulation). High-magnification SEM imaging (no stimulation) further revealed preferential interaction of the PC12 cells to the PEDOT:PSS nanoparticle arrays, confirming not only biocompatibility with the large

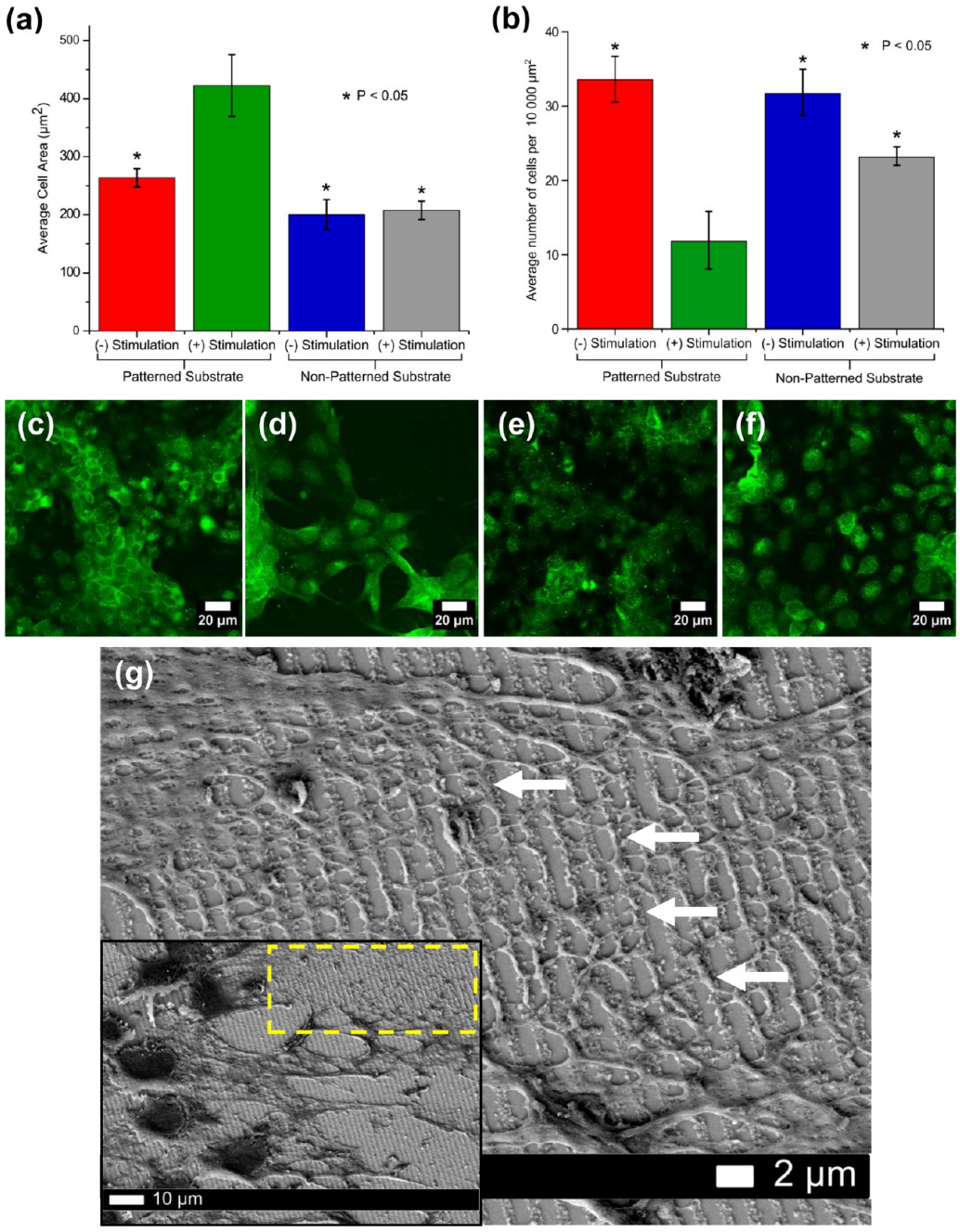

Figure 4. Exogenous electrical stimulation induced dendritic sprouting of the PC12 cells guided by the PEDOT:PSS linear conduits. (a) Significant increase in the average cell area is observed 72 h after exogenous electrical stimulation on the nanoparticle platform in comparison to unstimulated and nonpatterned controls. (b) Corresponding decrease in PC12 cell proliferation observed 72 h after exogenous electrical stimulation on the nanoparticle platform in comparison to unstimulated and nonpatterned controls. (c−f) Representative confocal images (40× magnification) of β-III tubulin immunohistochemically stained cells 72 h after the following treatments: {(+) pattern, (−) stimulation} (c); {(+) pattern, (+) stimulation} (d); {(−) pattern, (−) stimulation} (e); {(−) pattern, (+) stimulation} (f), demonstrating modulation of cell morphology. (g) High-magnification SEM image (magnification 8k×) indicating the formation of extensive dendritic networks (white arrows) guided by the PEDOT:PSS arrays. Inset: The corresponding low-magnification image of the area (yellow box) analyzed (magnification 3k×).

area of the pattern but also potential applicability of the nanoscale linear arrays as guidance conduits (Figure 3c).

Exogenous Electrical Stimulation Induced Dendritic Sprouting of the PC12 Cells. Electrical stimulation has been effectively used to modulate growth and differentiation of anchorage-dependent cells such as neurons, fibroblasts, and epithelium cells.[17,20,21] In the central nervous system, brief stimulation to the proximal end of transected peripheral nerves has been shown to augment preferential motor reinnervation,[22] improve the specificity of sensory reinnervation,[23] and accelerate

the reinnervation of distal target tissues.[24] These have been reported to depend on depolarization of the neuronal soma and its axon, involvement of axon guidance factors such as polysilylated neural cell adhesion molecule,[25] the L2/HNK-1 carbohydrate,[26] and brain-derived neurotrophic factor.[27] Finally electrical stimulation induced neurite outgrowth was recently reported to be dependent on calcium influx through L- and N-type voltage-dependent calcium channels and calcium mobilization from IP3R and RYR-sensitive calcium stores.[28] In the present case, we analyzed the morphological modulation of PC12 cells following electrical stimulation having determined no change in cell viability using the MTS assay. Nerve growth factor (NGF) induces PC12 cells to change their phenotype and acquire a number of properties that are similar to sympathetic neurons. Importantly, although they can acquire properties similar to sympathetic neurons upon NGF treatment, they do not develop definitive dendritic axons or form true synapses with each other in the absence of exogenous stimulation.[29] This change in phenotype upon NGF treatment is associated with a retardation in proliferation, the extension of neurites making them electrically excitable. Monitoring the cell numbers and cell area can assess this change from the proliferation state to a differentiation state. Furthermore, microtubule levels correlate precisely with the neurite extension during NGF-induced PC12 cell differentiation.[29,30] Using immunohistochemical staining for β-III tubulin it was determined that stimulation on the patterned surface resulted in a significant increase in the cell area and lower number of cells per unit area, indicating exogenous electrical stimulation induced differentiation of PC12 cells (Figure 4a–f, Figure S4). High-magnification SEM (Figure 4g) also revealed that stimulation resulted in an extensive dendritic network guided by the linear conduits of PEDOT:PSS nanoparticles.

CONCLUSION

In summary, we have demonstrated a practical and transferable protocol to fabricate self-assembled large-area patterns of conducting polymers from solution. This overcomes some of the shortfalls in the current fabrication techniques in developing patterned organic bionic devices. The patterns generated have demonstrated excellent biocompatibility. At the same time, they have been shown to induce exogenous electrical stimulation under physiological conditions to elicit a measurable and consistent cellular response. Importantly the methodology permits the design of bionic devices capable of inducing local electrical stimulation for *in vivo* applications while integrating multimodal imaging and simultaneous drug delivery capabilities of nanoparticles.

METHODS SUMMARY

Nanoparticle Synthesis. The conducting nanoparticles were prepared *via* a nonspontaneous emulsification route. Briefly, rhodamine B was attached to PGMA in MEK at 80 °C under N_2 for 5 h. The modified PGMA was then precipitated in diethyl ether and dried under N_2. This was dispersed in a 1:3 mixture of $CHCl_3$ and MEK along with 25 mg of Fe_3O_4 to form the organic phase. This organic phase was added dropwise into a rapidly stirring aqueous solution of Pluronic F-108. The emulsion was homogenized with a probe-type ultrasonic wand for 1 min. The organic solvents were then evaporated off under N_2. Large aggregates of Fe_3O_4 and excess polymer were separated *via* centrifugation. The nanoparticles in the supernatant were then mixed with PEI and heated to 80 °C for 16 h to facilitate attachment. The PEI-coated nanoparticles were isolated and washed on a magnetic separation column. Next, a diluted solution of PEDOT:PSS was added dropwise under rapid stirring to nanoparticles at a concentration of 0.5 mg/mL to facilitate electrostatic attachment. This was followed by sonication for 10 min and stirring for 18 h. The nanoparticles were then washed multiple times in water before being stored at 4 °C for further use.

Platform Fabrication. To direct the self-assembly of the nanoparticles, a template was fabricated by CFL. A 0.2% w/v PGMA in $CHCl_3$ solution was spin coated on ITO coverslips and annealed at 120 °C for 20 min. Next, 1.3% w/v PS in toluene was spin coated onto the PGMA surface. A PDMS stamp was then placed onto the PS layer, followed by heat treatment in an oven at 130 °C for 1 h. Once cooled, the stamp was peeled off. This was followed by exposure to EA at room temperature for 5 h. The pattern was next washed multiple times with water to remove unreacted EA. A 50 μL amount of 4 mg/mL nanoparticle suspension was drop casted onto the patterned area of the coverslip. The setup was then placed in a sealed vial, facilitating controlled evaporation, which allowed for electrostatic nanoparticle attachment onto the EA surface. The PS mask was then removed by washing with toluene. The resulting patterned PEDOT:PSS nanoparticle array was then used for further experimentation.

Electrical Stimulation Protocol. For electrical stimulation experiments, two silver epoxy electrodes were painted onto the ends of the patterned nanoparticle arrays. Prior to cell culture, the whole platform was UV and ethanol sterilized. Wells were coated with poly(L-lysine) and 15 μg/mL of laminin followed by cell seeding at a density of 50 000 cells/well. Cells were left to adhere for 18 h. Immediately prior to stimulation, the proliferation media was replaced with low-serum nerve growth factor containing differentiation media. For stimulation, the cells were subjected to a monophasic pulsed current at a frequency of 250 Hz with a 2 ms pulse width and an amplitude of 1 mA for 2 h, after which they were left for an additional 72 h before analysis.

Cell Viability Assessment. Cell viability was measured using the MTS assay as per the manufacturer protocols (Invitrogen, UK). For measurements, 80 μL from each well was transferred into a new 96-well plate and read under a plate reader at 490 nm excitation wavelength. To analyze cell morphology, cells were immunohistochemically stained for β-III tubulin.

Material Characterization. AFM was performed on a Dimension 3100 AFM system with a Nanoscope IV controller used to obtain the AFM images in tapping mode, using Pt/Ir-coated contact mode probes with a spring constant of 0.2 N/m (type SCM-PIC, Bruker). TEM was performed on a JEOL 2100 transmission electron microscope at an accelerating voltage of 80 kV. SEM was performed on a Zeiss 1555 VP-FESEM, and all samples were coated with 5 nm of Pt. Biological samples were initially fixed in 2.5% glutaraldehyde and dehydrated in increasing concentrations of ethanol followed by critical point drying prior to Pt coating. Immunohistochemically stained samples were

analyzed using a Leica TCS SP2 AOBS multiphoton confocal microscope.

Conflict of Interest: The authors declare no competing financial interest.

Supporting Information Available: Detailed materials and methods: synthesis, characterization (TEM, SEM, AFM), cell culture, and electrical stimulation experiments. This material is available free of charge *via* the Internet at http://pubs.acs.org.

Acknowledgment. D.H., I.L., and K.S.I. designed the experiments, developed the concept, and analyzed the data. D.H., J.Z., and N.M.S. optimized the capillary force lithography experiments. D.H., X.C., V.A., and A.M. performed image acquisition using confocal microscopy, transmission electron microscopy, scanning electron microscopy, and atomic force microscopy. D.H., A.R.H., G.W.P., S.I.H., and A.B. optimized and designed the electrical stimulation experiments. This work was funded by the Australian Research Council (ARC), the National Health & Medical Research Council (NHMRC) of Australia, and the National Science Foundation (CBET-0756457). The authors acknowledge the Australian Microscopy & Microanalysis Research Facility at the Centre for Microscopy, Characterization & Analysis, and The University of Western Australia, funded by the University, State and Commonwealth Governments. The authors also wish to thank Margaret Pollett and Chrisna LeVaillant for their invaluable contribution in assisting with the PC12 cell cultures and immunohistochemistry, and Ella Marushchenko (www.scientific-illustrations.com) for assistance with Figure 1.

REFERENCES AND NOTES

1. Ciofani, G.; Danti, S.; D'Alessandro, D.; Ricotti, L.; Moscato, S.; Bertoni, G.; Falqui, A.; Berrettini, S.; Petrini, M.; Mattoli, V.; *et al*. Enhancement of Neurite Outgrowth in Neuronal-Like Cells Following Boron Nitride Nanotube-Mediated Stimulation. *ACS Nano* **2010**, *4*, 6267–6277.
2. Moulton, S. E.; Higgins, M. J.; Kapsa, R. M. I.; Wallace, G. G. Organic Bionics: A New Dimension in Neural Communications. *Adv. Funct. Mater.* **2012**, *22*, 2003–2014.
3. Wallace, G. G.; Moulton, S. E.; Clark, G. M. Electrode-Cellular Interface. *Science* **2009**, *324*, 185–186.
4. Wallace, G. G.; Higgins, M. J.; Moulton, S. E.; Wang, C. Nanobionics: The Impact of Nanotechnology on Implantable Medical Bionic Devices. *Nanoscale* **2012**, *4*, 4327–4347.
5. Khademhosseini, A.; Langer, R.; Borenstein, J.; Vacanti, J. P. Microscale Technologies for Tissue Engineering and Biology. *Proc. Natl. Acad. Sci. U.S.A.* **2006**, *103*, 2480–2487.
6. Guimard, N. K.; Gomez, N.; Schmidt, C. E. Conducting Polymers in Biomedical Engineering. *Prog. Polym. Sci.* **2007**, *32*, 876–921.
7. Kim, D. H.; Richardson-Burns, S. M.; Hendricks, J. L.; Sequera, C.; Martin, D. C. Effect of Immobilized Nerve Growth Factor on Conductive Polymers: Electrical Properties and Cellular Response. *Adv. Funct. Mater.* **2007**, *17*, 79–86.
8. Lee, J. I.; Cho, S. H.; Park, S.-M.; Kim, J. K.; Kim, J. K.; Yu, J.-W.; Kim, Y. C.; Russell, T. P. Highly Aligned Ultrahigh Density Arrays of Conducting Polymer Nanorods Using Block Copolymer Templates. *Nano Lett.* **2008**, *8*, 2315–2320.
9. Wang, J.; Zheng, Z.; Li, H.; Huck, W.; Sirringhaus, H. Dewetting of Conducting Polymer Inkjet Droplets on Patterned Surfaces. *Nat. Mater.* **2004**, *3*, 171–176.
10. Nakashima, H.; Higgins, M. J.; O'Connell, C.; Torimitsu, K.; Wallace, G. G. Liquid Deposition Patterning of Conducting Polymer Ink onto Hard and Soft Flexible Substrates *via* Dip-Pen Nanolithography. *Langmuir* **2011**, *28*, 804–811.
11. Iyer, K. S.; Zdyrko, B.; Malz, H.; Pionteck, J.; Luzinov, I. Polystyrene Layers Grafted to Macromolecular Anchoring Layer. *Macromolecules* **2003**, *36*, 6519–6526.
12. Zou, J.; Zdyrko, B.; Luzinov, I.; Raston, C. L.; Swaminathan Iyer, K. Regiospecific Linear Assembly of Pd Nanocubes for Hydrogen Gas Sensing. *Chem. Commun.* **2012**, *48*, 1033–1035.
13. Choi, J.; Lee, J.; Jung, D.; Shim, S. E. Electrospun PEDOT: PSS/PVP Nanofibers as the Chemiresistor in Chemical Vapour Sensing. *Synth. Met.* **2010**, *160*, 1415–1421.
14. Merrill, D. R.; Bikson, M.; Jefferys, J. G. R. Electrical Stimulation of Excitable Tissue: Design of Efficacious and Safe Protocols. *J. Neurosci. Methods* **2005**, *141*, 171–198.
15. Chen, C. S.; Mrksich, M.; Huang, S.; Whitesides, G. M.; Ingber, D. E. Micropatterned Surfaces for Control of Cell Shape, Position, and Function. *Biotechnol. Prog.* **1998**, *14*, 356–363.
16. Ito, Y. Surface Micropatterning to Regulate Cell Functions. *Biomaterials* **1999**, *20*, 2333–2342.
17. Schmidt, C. E.; Shastri, V. R.; Vacanti, J. P.; Langer, R. Stimulation of Neurite Outgrowth Using an Electrically Conducting Polymer. *Proc. Natl. Acad. Sci. U.S.A.* **1997**, *94*, 8948–8953.
18. Richardson, R. T.; Thompson, B.; Moulton, S.; Newbold, C.; Lum, M. G.; Cameron, A.; Wallace, G.; Kapsa, R.; Clark, G.; O'Leary, S. The Effect of Polypyrrole with Incorporated Neurotrophin-3 on the Promotion of Neurite Outgrowth from Auditory Neurons. *Biomaterials* **2007**, *28*, 513–523.
19. Weng, B.; Liu, X.; Shepherd, R.; Wallace, G. G. Inkjet Printed Polypyrrole/Collagen Scaffold: A Combination of Spatial Control and Electrical Stimulation of PC12 Cells. *Synth. Met.* **2012**, *162*, 1375–1380.
20. Wong, J. Y.; Langer, R.; Ingber, D. E. Electrically Conducting Polymers Can Noninvasively Control the Shape and Growth of Mammalian Cells. *Proc. Natl. Acad. Sci. U.S.A.* **1994**, *91*, 3201–3204.
21. Bourguignon, G.; Bourguignon, L. Electric Stimulation of Protein and DNA Synthesis in Human Fibroblasts. *FASEB J.* **1987**, *1*, 398–402.
22. Al-Majed, A. A.; Neumann, C. M.; Brushart, T. M.; Gordon, T. Brief Electrical Stimulation Promotes the Speed and Accuracy of Motor Axonal Regeneration. *J. Neurosci.* **2000**, *20*, 2602–2608.
23. Brushart, T. M.; Jari, R.; Verge, V.; Rohde, C.; Gordon, T. Electrical Stimulation Restores the Specificity of Sensory Axon Regeneration. *Exp. Neurol.* **2005**, *194*, 221–229.
24. Brushart, T. M.; Hoffman, P. N.; Royall, R. M.; Murinson, B. B.; Witzel, C.; Gordon, T. Electrical Stimulation Promotes Motoneuron Regeneration without Increasing Its Speed or Conditioning the Neuron. *J. Neurosci.* **2002**, *22*, 6631–6638.
25. Franz, C. K.; Rutishauser, U.; Rafuse, V. F. Intrinsic Neuronal Properties Control Selective Targeting of Regenerating Motoneurons. *Brain* **2008**, *131*, 1492–1505.
26. Eberhardt, K. A.; Irintchev, A.; Al-Majed, A. A.; Simova, O.; Brushart, T. M.; Gordon, T.; Schachner, M. BDNF/TrkB Signaling Regulates HNK-1 Carbohydrate Expression in Regenerating Motor Nerves and Promotes Functional Recovery after Peripheral Nerve Repair. *Exp. Neurol.* **2006**, *198*, 500–510.
27. Geremia, N. M.; Gordon, T.; Brushart, T. M.; Al-Majed, A. A.; Verge, V. M. Electrical Stimulation Promotes Sensory Neuron Regeneration and Growth-Associated Gene Expression. *Exp. Neurol.* **2007**, *205*, 347–359.
28. Yan, X.; Liu, J.; Huang, J.; Huang, M.; He, F.; Ye, Z.; Xiao, W.; Hu, X.; Luo, Z. Electrical Stimulation Induces Calcium-Dependent Neurite Outgrowth and Immediate Early Genes Expressions of Dorsal Root Ganglion Neurons. *Neurochem. Res.* **2014**, *39*, 129–141.
29. Das, K. P.; Freudenrich, T. M.; Mundy, W. R. Assessment of PC12 Cell Differentiation and Neurite Growth: A Comparison of Morphological and Neurochemical Measures. *Neurotoxicol. Teratol.* **2004**, *26*, 397–406.
30. Drubin, D. G.; Feinstein, S. C.; Shooter, E. M.; Kirschner, M. W. Nerve Growth Factor-Induced Neurite Outgrowth in PC12 Cells Involves the Coordinate Induction of Microtubule Assembly and Assembly-Promoting Factors. *J. Cell Biol.* **1985**, *101*, 1799–1807.